CUL-2 and ZYG-11 promote meiotic anaphase II and the proper placement of the anterior-posterior axis in *C. elegans*

Ji Liu*, Srividya Vasudevan* and Edward T. Kipreos†

Department of Cellular Biology, University of Georgia, Athens, GA 30602-2607, USA
*These authors contributed equally to this work
†Author for correspondence (e-mail: ekipreos@cb.uga.edu)

Accepted 30 April 2004

Development 131, 3513-3525
Published by The Company of Biologists 2004
doi:10.1242/dev.01245

Summary

The faithful segregation of chromosomes during meiosis is vital for sexual reproduction. Currently, little is known about the molecular mechanisms regulating the initiation and completion of meiotic anaphase. We show that inactivation of CUL-2, a member of the cullin family of ubiquitin ligases, delays or abolishes meiotic anaphase II with no effect on anaphase I, indicating differential regulation during the two meiotic stages. In *cul-2* mutants, the cohesin REC-8 is removed from chromosomes normally during meiosis II and sister chromatids separate, suggesting that the failure to complete anaphase results from a defect in chromosome movement rather than from a failure to sever chromosome attachments. CUL-2 is required for the degradation of cyclin B1 in meiosis and inactivation of cyclin B1 partially rescued the meiotic delay in *cul-2* mutants. In *cul-2* mutants, the failure to degrade cyclin B1 precedes the metaphase II arrest. CUL-2 is also required for at least two aspects of embryonic polarity. The extended meiosis II in *cul-2* mutants induces polarity reversals that include reversed orientation of polarity proteins, P granules, pronuclei migration and asymmetric cell division. Independently of its role in meiotic progression, CUL-2 is required to limit the initiation/spread of the polarity protein PAR-2 in regions distant from microtubule organizing centers. Finally, we show that inactivation of the leucine-rich repeat protein ZYG-11 produces meiotic and polarity reversal defects similar to those observed in *cul-2* mutants, suggesting that the two proteins function in the same pathways.

Key words: PAR-2, CUL2, Cullin, Polarity, Meiosis, Metaphase II, *C. elegans*

Introduction

The faithful segregation of chromosomes during meiosis is vital for sexual reproduction, as missegregation leads to aneuploidy. Meiotic chromosome segregation involves two processes: loss of cohesion between chromosome homologs and the movement of chromosomes to opposite spindle poles. The molecular mechanisms that regulate meiotic chromosome cohesion are relatively well understood. Central to chromosome cohesion is the REC-8 cohesin complex, which holds chromosomes together from premeiotic S phase until anaphase (Petronczki et al., 2003). In budding and fission yeast, Rec8 is cleaved during meiosis I by separase in non-centromeric regions to allow the separation of chromosome homologs (Buonomo et al., 2000; Kitajima et al., 2003). In meiosis II, the remaining centromeric Rec8 is removed to allow sister chromatid separation, and this has been shown to require separase activity in fission yeast (Kitajima et al., 2003). In *C. elegans*, REC-8 is partially removed from chromosomes at anaphase I and is completely removed at anaphase II (Pasierbek et al., 2001). Inactivation of a *C. elegans* separase homolog leads to a failure of chromosome separation, suggesting that the cohesin degradation mechanism is conserved (Siomos et al., 2001). In contrast to the detailed information about chromosome cohesion and its dissolution, little is known about the mechanisms that regulate chromosome movement during meiotic anaphase.

In many metazoa, the anteroposterior (AP) body axis is defined at a very early stage, when patterning molecules are asymmetrically distributed in the embryo (Pellettieri and Seydoux, 2002). In the nematode *C. elegans*, AP polarity is initiated in the zygote immediately after meiosis by the sperm pronucleus/centrosome complex (SPCC) (Goldstein and Hird, 1996). In response to the SPCC, the PDZ-domain polarity protein PAR-6 becomes excluded from the posterior cortex. PAR-6 functions in a complex with the PDZ-domain protein PAR-3 and the atypical protein kinase C PKC-3 (Tabuse et al., 1998; Hung and Kemphues, 1999; Joberty et al., 2000). The exclusion of PAR-6 from the posterior allows the RING finger protein PAR-2 to accumulate on the posterior cortex (Watts et al., 1996; Boyd et al., 1996; Hung and Kemphues, 1999; Cuenca et al., 2003). This redistribution of PAR-2 and PAR-6 is required for subsequent AP asymmetries, including the polarized localization of maternal proteins to specify different cell fates and the asymmetric orientation of the mitotic spindle to generate unequal cell divisions (Schneider and Bowerman, 2003; Pellettieri and Seydoux, 2002).

Ubiquitin-mediated protein degradation is an essential aspect of many dynamic cellular processes, including cell cycle progression, signal transduction and transcription (Pickart, 2001). The covalent attachment of poly-ubiquitin chains to proteins can signal degradation by the 26S proteasome (Pickart, 2001). The addition of ubiquitin to proteins is highly

regulated and requires the action of an ubiquitin-activating enzyme (E1), an ubiquitin-conjugating enzyme (E2) and an ubiquitin ligase (E3). The substrate specificity of ubiquitination derives from the recognition of the substrate by the ubiquitin ligase. A major class of E3s is the cullin/RING finger ubiquitin ligases (Tyers and Jorgensen, 2000). The cullin gene family comprises five major groupings in metazoa, CUL-1 through CUL-5 (Tyers and Jorgensen, 2000). In mammals, CUL2 functions in an E3 complex that contains the core components elongin C, elongin B and the RING-H2 finger protein RBX1/ROC1 (Kim and Kaelin, 2003).

Here, we show that CUL-2, as well as orthologs of elongin C and RBX1, is required for the initiation of meiotic anaphase II but not for anaphase I. The meiotic delay in *cul-2* mutants causes a reversal of AP polarity. By titrating the length of the delay, we demonstrate that there is a tight linkage between meiotic timing and the placement of the AP axis. We also show that CUL-2 has an additional role to prevent the ectopic localization or spreading of PAR-2 on the cortex.

Materials and methods

Strains and alleles

C. elegans strains were cultured as previously described (Brenner, 1974). Strains and alleles used were: Bristol N2; AZ212 [*unc-119(ed3)*; ruIs32 (pAZ132: *pie-1* promoter/histone H2B::GFP)]; AZ244 [*unc-119(ed3)*; ruIs57 (pAZ147: *pie-1* promoter/β-tubulin::GFP; *unc-119(+)*)]; KK866 [itIs153 (*pie-1* promoter/PAR-2::GFP, pRF4, N2 genomic DNA)]; JH1461 [axEx1121 (*pie-1* promoter/PAR-6::GFP, pRF4, N2 DNA)]; JH1473 [itIs153; ruIs57]; ET108 [*cul-2(ek1)/unc-64(e246)*; ruIs32]; ET129 [*unc-119(ed3)*; itIs153; ruIs32]; DG627 [*emb-30(tn377*ts)]; ET143 [*zyg-11(mn40) unc-4(e120)/mnC1; cul-2(ek1)/unc-64(e246)*]; ET144 [*zyg-11(mn40) unc-4(e120)/mnC1; cul-2(ek1)/unc-64(e246)*; ruIs32]; SP152 [*him-1(e879); zyg-11(mn40) unc-4(e120)/mnC1*]; ET155 [*zyg-11(mn40) unc-4(e120)/mnC1*; ruIs32]; and ET113 [*unc-119(ed3)*; ekIs2 (*pie-1* promoter/CYB-1::GFP; *unc-119(+)*)]. N2 and ET108 were maintained at 20°C, DG627 was maintained at 15°C, and all other strains were maintained at 24°C.

RNAi

RNAi was performed either by injection of dsRNA into hermaphrodites or by feeding with bacteria expressing dsRNA, as described (Feng et al., 1999; Timmons et al., 2001). To produce a partial loss of CUL-2 function, embryos were observed between 4 and 12 hours post-injection of *cul-2* dsRNA into adult hermaphrodites. The *cul-2; rec-8* double RNAi experiment followed the protocol of Davis et al. (Davis et al., 2002), except that after injection of *rec-8* dsRNA into adult hermaphrodites, L4-stage progeny were placed on *cul-2* RNAi bacteria feeding plates for 24 hours prior to observation. Inactivation of *cul-2* in double RNAi experiments was assessed by observation of the multinuclei and cytoplasmic extensions that occur in *cul-2* mutant embryos (Feng et al., 1999). The effectiveness of *cyb-1* RNAi was confirmed by the elimination of CYB-1::GFP signal.

Microscopy

Time-lapse movies were made of embryos in utero. Young adult hermaphrodites were anesthetized either with 0.1% tricaine, 0.01% tetramisole (Sigma) in M9 solution or 10 mM levamisole (Sigma) in M9 solution. To observe the initiation of PAR-2 cortical localization, zygotes were cut from the uterus into EBGM medium (Shelton and Bowerman, 1996) on 12×12 mm coverslips. The coverslip was mounted on 4% agarose pads with a thin layer of petroleum jelly applied between the coverslip and the pad to eliminate pressure on the zygotes. Automatic time-lapse imaging was performed with a Zeiss Axioplan microscope equipped with a Hamamatsu ORCA-ER CCD camera, LUDL hardware controller, automated filter wheels and shutters, and an Apple G4 computer running Openlab software (Improvision). Movies were made with pulsed 100 msec exposures for DIC and epifluorescence every 40-80 seconds; epifluorescent illumination was from a 100 W HBO mercury lamp that was filtered to 25% of normal levels. PAR-2::GFP cortical patches were only scored when they were of higher epifluorescent intensity than the interior cytoplasm, except in Table 2 where they were noted as being transient and weak. For the timing of meiosis I, the following number of embryos were observed: wild type, *n*=5; *cul-2(RNAi)*, *n*=5; *cul-2(ek1)*, *n*=5; *elc-1(RNAi)*, *n*=3; *rbx-1(RNAi)*, *n*=4; *elb-1(RNAi)*, *n*=6; *zyg-11(RNAi)*, *n*=9; *zyg-11(mn40)*, *n*=3; and *zyg-11(mn40); cul-2(ek1)*, *n*=5. For the timing of meiosis II, the following number of embryos were observed: wild type, *n*=5; *cul-2(RNAi)*, *n*=5; *cul-2(ek1)*, *n*=5; *elc-1(RNAi)*, *n*=5; *rbx-1(RNAi)*, *n*=4; *elb-1(RNAi)*, *n*=9; *zyg-11(RNAi)*, *n*=9; *zyg-11(mn40)*, *n*=4; and *zyg-11(mn40); cul-2(ek1)*, *n*=5. Quantitation of CYB-1::GFP levels was performed by measuring the fluorescent signal with OpenLab software and subtracting background fluorescence.

The following primary antibodies were used for immunofluorescence: anti-REC-8 (Pasierbek et al., 2001); anti-PAR-2 (Boyd et al., 1996); anti-PAR-6 (Hung and Kemphues, 1999); anti-P granules, OI1CD4 (Strome and Wood, 1982) and monoclonal 4G8 (J.L., S.V. and E.T.K., unpublished); anti-α-tubulin (N356, Amersham); and anti-GFP, 3E6 (Molecular Probes) and ab6556 (AbCam). Secondary antibodies used were: anti-mouse rhodamine (Cappel); and anti-rabbit Alexa Fluor 488 (Molecular Probes). Slides were incubated with 1 μg/ml DAPI to stain DNA prior to mounting in 90% glycerol/PBS with 1 mg/ml p-phenylenediamine (Sigma). The anti-α-tubulin and DAPI-stained meiotic spindle images were obtained as 0.3 μm z-sections and processed with Openlab multi-neighbor deconvolution software. For *emb-30(tn377)* immunofluorescence experiments, only zygotes that were arrested in meiosis I with the meiotic spindle associated with the anterior cortex and with no sperm asters were scored for PAR-2 and PAR-6 localization; this represents relatively younger arrest embryos prior to the wandering of the meiotic spindle or the formation of sperm asters. Images were processed with Adobe Photoshop software (6.0). The χ^2 test was used to determine statistical significance. Means are given with s.e.m.

Results

CUL-2 is required for meiotic anaphase II

Following fertilization in wild-type zygotes, the six maternal chromosome bivalents align in a pentagonal array at metaphase I (Albertson and Thomson, 1993) (Fig. 1A). In anaphase I, homologs segregate and a 2N polar body is extruded from the zygote. In metaphase II, the remaining six sister chromatids again adopt a pentagonal array (Fig. 1A). After the second polar body is extruded from the zygote, the maternal chromatids decondense, marking the completion of meiosis.

We examined meiotic chromosome dynamics using time-lapse movies of chromosomes visualized by transgenic expression of histone H2B::GFP. Zygotes homozygous for the *cul-2(ek1)* null allele (Feng et al., 1999) and zygotes depleted of CUL-2 by RNA-mediated interference *(RNAi)* (Fire et al., 1998) had indistinguishable phenotypes. They both completed meiosis I with normal chromosome dynamics approximately 15 minutes post-fertilization, similar to wild type (Fig. 1A,B). Significantly, while meiosis II lasted approximately 15 minutes in wild type, it took an average of 50 to 60 minutes in *cul-2(RNAi)* and *cul-2(ek1)* zygotes (Fig. 1A,B). Afterwards,

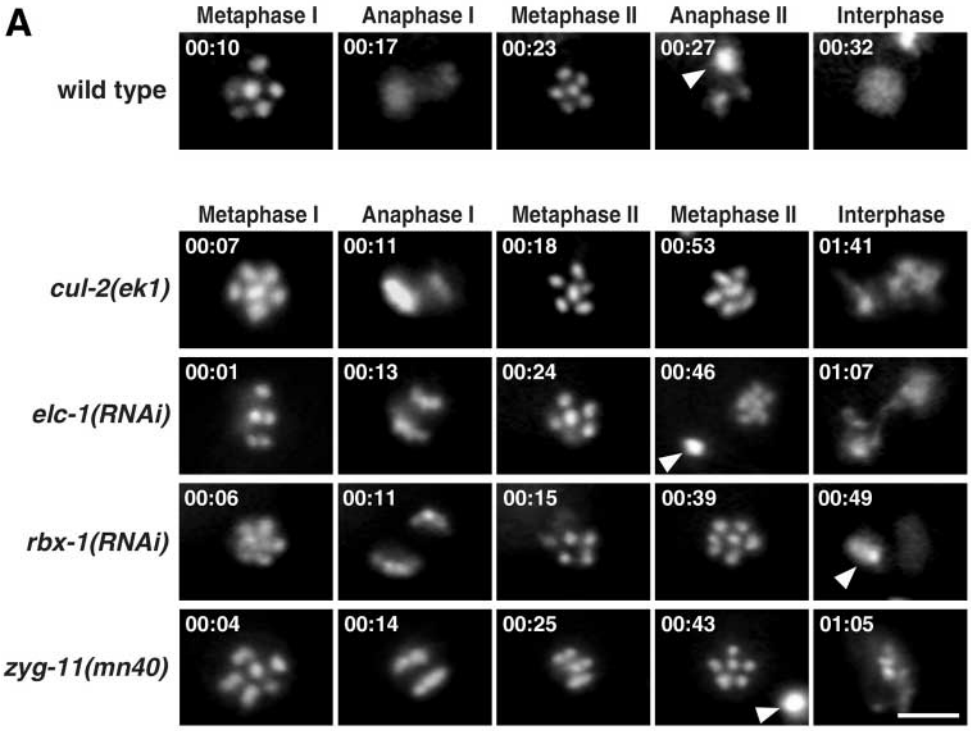

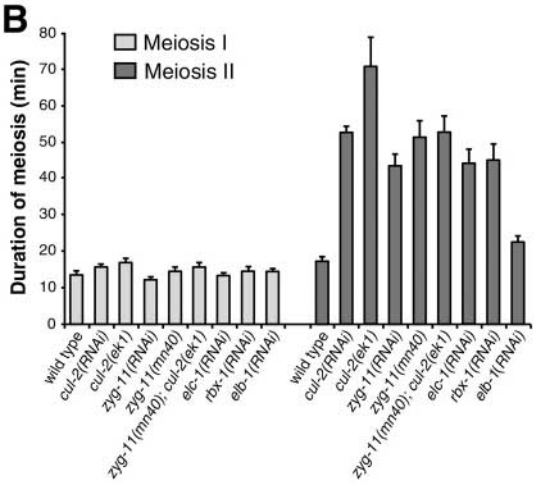

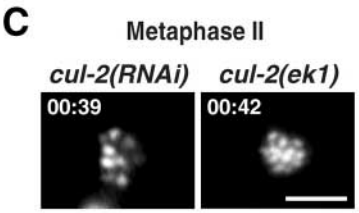

Fig. 1. CUL-2 complex components and ZYG-11 are required for progression into meiotic anaphase II. (A) Histone H2B::GFP epifluorescence movie sequences of live zygotes of the indicated genotype. Time post-fertilization is indicated in the upper left corner (hours:minutes). Interphase denotes the initiation of chromosome decondensation after meiotic exit. The metaphase images are generally transverse views to show the pentagonal array except for the *elc-1* (00:01) and *zyg-11(mn40)* (00:25), which are side views showing paired homologous chromosomes and sister chromatids, respectively. Arrowheads denote polar bodies. (B) The duration of meiosis I post-fertilization (left) and meiosis II (right) derived from histone H2B::GFP movies. See Materials and methods for the number of embryos analyzed. (C) Histone H2B::GFP images of separated metaphase II chromosomes in *cul-2(RNAi)* and *cul-2(ek1)* embryos. Scale bars: 5 μm.

the chromosomes generally congressed and individual chromosomes could not be discerned; this was followed by decondensation. Of 18 zygotes observed, ten never executed anaphase II (Fig. 1A), whereas in the other eight the DNA split immediately before or after chromosome decondensation, with DNA bridges observed in the majority of cases (7/8). RNAi depletion of *elc-1* and *rbx-1*, the orthologs of mammalian CUL-2 complex components elongin C and RBX1/ROC1, respectively, produced metaphase II arrest phenotypes similar to that of *cul-2* mutants (Fig. 1A,B). This suggests that CUL-2 normally promotes entry into anaphase in the context of a conserved ubiquitin ligase complex.

cul-2 and *zyg-11* mutants have a similar meiosis II arrest

The failure of *cul-2* mutant embryos to initiate anaphase II was reminiscent of the *zyg-11* mutant phenotype. In a study by Kemphues et al. (Kemphues et al., 1986), embryos homozygous for the hypomorphic allele *zyg-11(bn2)* were found to progress through meiosis I with normal timing, whereas the time for meiosis II was extended to 26 minutes. We analyzed embryos homozygous for the null allele *zyg-11(mn40)*, as well as *zyg-11(RNAi)* embryos, and found a longer meiosis II delay of 50.2±4.0 minutes (n=5) and 43.6±3.1 minutes (n=9), respectively, comparable to the delay observed in *cul-2* mutants (Fig. 1A,B). To test whether simultaneous inactivation of both genes increased the severity of the meiotic arrest, as might occur if the two genes affected meiotic progression through independent pathways, we created a double heterozygous mutant strain (ET144) using null alleles for each gene. Double homozygous *zyg-11(mn40); cul-2(ek1)* embryos from this strain remained in meiosis II for 53±4.5 minutes (n=5), equivalent to the timings seen upon individual inactivation of each gene (Fig. 1B). This result is consistent with the two genes functioning in the same pathway to regulate anaphase II.

In addition to defective meiosis II, *zyg-11* and *cul-2* mutant embryos share other phenotypes, including the presence of multinuclei and cytoplasmic extensions during mitotic division (Feng et al., 1999; Kemphues et al., 1986). One difference between the two mutants is the presence of G1-phase arrested germ cells in *cul-2* mutants (Feng et al., 1999), which are not

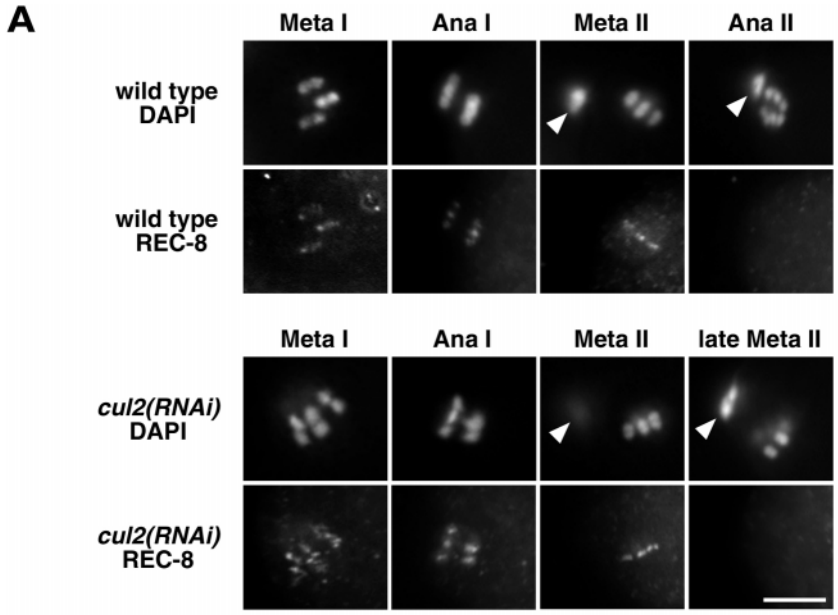

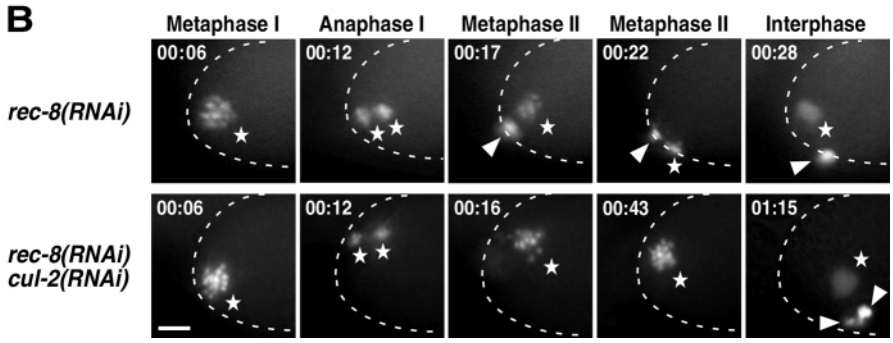

Fig. 2. The *cul-2* meiotic phenotypes are not caused by a failure to remove the cohesin REC-8 from sister chromatids. (A) Immunofluorescence images of REC-8 in wild-type and *cul-2(RNAi)* embryos. Images of wild-type (top) and *cul-2(RNAi)* zygotes (bottom) stained with DAPI and anti-REC-8 antibody at the indicated meiotic stages. Note that in late metaphase II *cul-2(RNAi)* zygotes, REC-8 is not detected but chromosomes fail to segregate. Arrowheads indicate polar bodies. (B) Depletion of *rec-8* by RNAi does not rescue the meiotic delay in *cul-2(RNAi)* zygotes. Histone H2B::GFP fluorescence movie sequences in *rec-8(RNAi)* or *cul-2(RNAi)*; *rec-8(RNAi)* double RNAi embryos. In the *rec-8(RNAi)* zygote, chromosomes compress and rapidly move to the cell cortex between time points 00:17 and 00:22. Time from fertilization (hours:minutes) is shown in the upper left corner of images. Stars denote meiotic chromosomes or interphase pronuclei. Dashed lines denote the egg boundary; arrowheads denote polar bodies. Scale bars: 5 μm.

observed in *zyg-11* mutants. The decreased number of germ cells in *cul-2* mutants leads to a lower numbers of eggs. We sought to test whether combining the *cul-2* mutant with the *zyg-11* mutant would enhance the *cul-2* egg production defect. *zyg-11(mn40); cul-2(ek1)* double homozygotes produced a low number of eggs (35.2±4.7; *n*=18), which was comparable to the egg numbers in *cul-2(ek1)* homozygotes (Feng et al., 1999) or hermaphrodites that are homozygous for *cul-2(ek1)* and heterozygous for *zyg-11(mn40)* (29.3±5.5; *n*=19). Conversely, animals homozygous for *zyg-11(mn40)* but heterozygous for *cul-2(ek1)* had egg numbers (333±3.2; *n*=10) similar to wild type, indicating that the loss of *zyg-11* cannot induce a germline arrest phenotype in *cul-2(ek1)* heterozygotes. These results suggest that ZYG-11 is unlikely to function with CUL-2 in promoting germline proliferation.

CUL-2 is not required for the removal of REC-8 from sister chromatids

A failure to segregate chromosomes during meiosis could result from defects in either chromosome separation or chromosome movement. In yeast, cohesin degradation is sufficient for the initiation of anaphase chromosome segregation (Uhlmann et al., 2000). In *C. elegans*, RNAi depletion of the cohesion REC-8 produces chromosome separation at diakinesis (Pasierbek et al., 2001).

To determine whether REC-8 is removed from chromosomes in *cul-2(RNAi)* zygotes, we studied REC-8 localization using immunofluorescence with anti-REC-8 antibody (Pasierbek et al., 2001). We found that the anti-REC-8 staining pattern in *cul-2(RNAi)* zygotes was similar to that in wild type. For both wild-type and *cul-2(RNAi)* zygotes, REC-8 is located along the axes of sister chromatids during metaphase I, and is located at the junction of the sister chromatids during metaphase II (Fig. 2A) (Pasierbek et al., 2001). In wild type, REC-8 is completely lost from the separating wild-type chromatids during anaphase II (Fig. 2A). In *cul-2(RNAi)* zygotes, although chromosomes remain in a metaphase II pentagonal array for an extended period, the majority of metaphase chromosomes do not have anti-REC-8 staining (70%, *n*=26; Fig. 2A). When *cul-2(RNAi)* zygotes are in the later stages of the extended meiosis II, the meiotic spindle often wanders away from the anterior pole of the egg. None of these late stage meiosis II zygotes were observed to have anti-REC8 staining (data not shown).

The lack of REC-8 staining suggests that the chromosomes in *cul-2(RNAi)* zygotes are not bound together. Indeed, we occasionally observed separated sister chromatids during the extended metaphase II of *cul-2* mutant zygotes (Fig. 1C). In 1/11 *cul-2(RNAi)* and 1/7 *cul-2(ek1)* mutants, approximately 12 individual chromatids were observed at the metaphase II plate rather than the normal six joined sister chromatids, indicating that cohesion had been lost between the sister chromatids, although chromosome segregation did not occur. A similar separation of sister chromatids during metaphase II is observed in *zyg-11(mn40)* mutant embryos (data not shown).

A further indication that a defect in chromosome cohesion was not responsible for the CUL-2 meiotic defects was

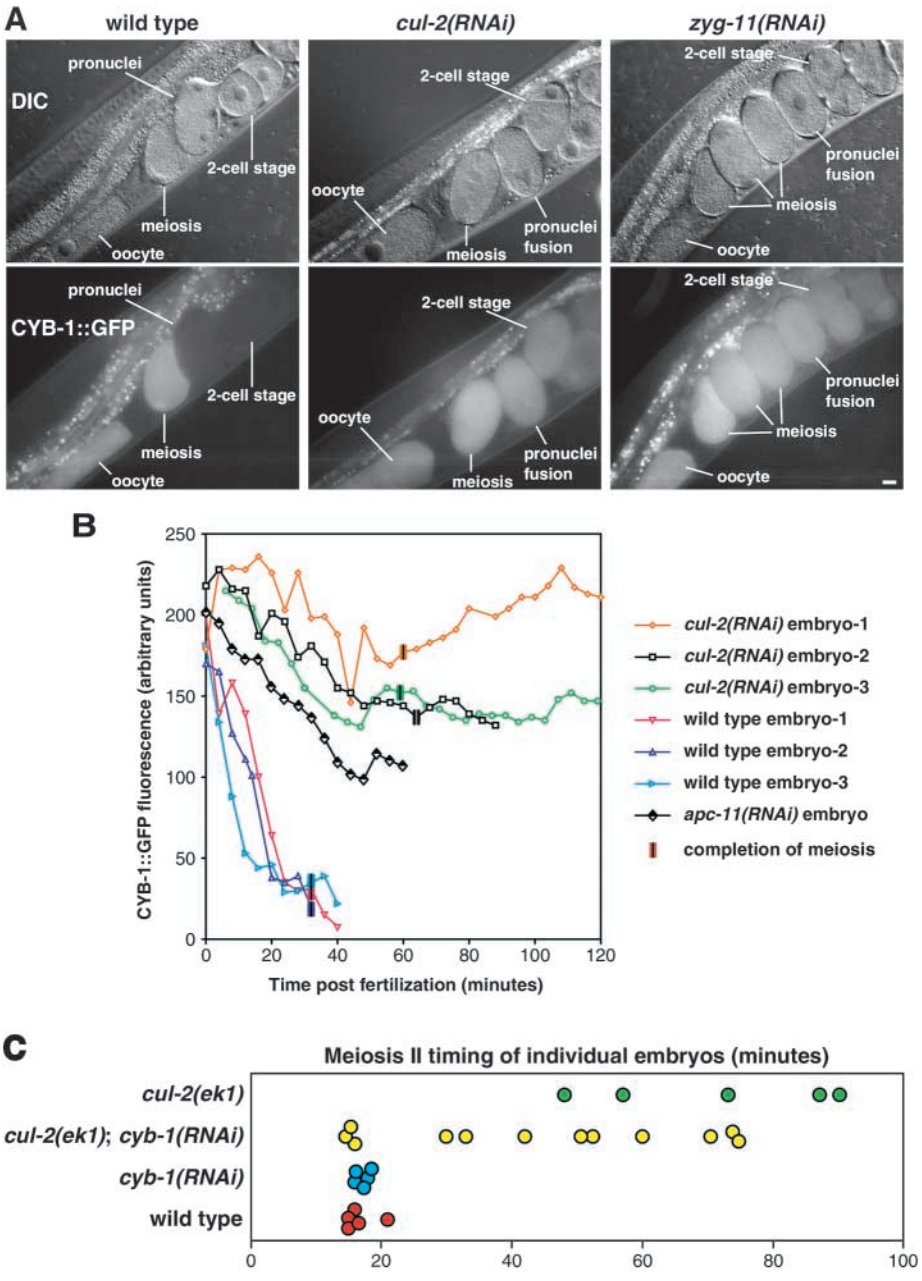

Fig. 3. Cyclin B1 is not degraded during meiosis in *cul-2(RNAi)* embryos. (A) DIC (top) and epifluorescence (bottom) images of wild-type, *cul-2(RNAi)* and *zyg-11(RNAi)* gravid adults expressing a *cyb-1*::GFP transgene. Embryo stages are labeled. Note that CYB-1::GFP signal is absent in the wild-type pronuclei stage embryo (immediately after meiosis) but perdures in *cul-2(RNAi)* and *zyg-11(RNAi)* embryos. Intestine autofluorescence is observed above the oocyte and eggs. Scale bar: 10 μm. (B) Graph of CYB-1::GFP epifluorescence intensity at times post-fertilization. Data was collected under the same conditions for each embryo and is presented in equivalent arbitrary units. The completion of meiosis is denoted by a thick striped bar. (C) Meiosis II timing for individual embryos of the strains listed, derived from histone H2B::GFP movies.

obtained from experiments in which zygotes were depleted of REC-8. Inactivation of REC-8 produces a loss of chromatid cohesion from the meiotic diakinesis stage onwards (Pasierbek et al., 2001). In both *rec-8(RNAi)* and *cul-2*; *rec-8* double RNAi zygotes, chromosomes segregate during anaphase I (Davis et al., 2002). However, in both zygotes we observed that chromosomes failed to segregate during meiosis II. Nevertheless, *rec-8(RNAi)* zygotes had normal meiosis II timing (16.1±0.7 minutes, *n*=9) (Fig. 2B). By contrast, *cul-2*; *rec-8* double RNAi zygotes had a meiosis II delay comparable to that observed in *cul-2(RNAi)* zygotes (55.2±6.5 minutes, *n*=4), indicating that the *cul-2* meiotic delay was not rescued by removing REC-8 (Fig. 2B).

An interesting observation was that in the majority of *rec-8(RNAi)* zygotes (7/8), a monopoleward movement of chromosomes toward the cortex was observed at the time when the second polar body would be extruded in wild type (Fig. 2B). The mechanistic basis of this monopoleward chromosome movement is not known, but it is similar to the chromosome behavior reported in *air-2(RNAi)* zygotes, which have a failure to remove REC-8 from meiotic chromosomes (Rogers et al., 2002). Interestingly, *cul-2*; *rec-8* double RNAi zygotes did not exhibit monopoleward chromosome movement (*n*=9), indicating that this aspect of meiotic chromosome movement was also defective (Fig, 2B).

Cyclin B1 is not degraded during meiosis in *cul-2(RNAi)* zygotes

The cyclin B/CDK1 complex is essential for entry and completion of mitosis and meiosis (Nebreda and Ferby, 2000). A failure to degrade cyclin B1 blocks the metaphase to anaphase transition in mitotically-dividing mammalian cells and is required for meiotic homolog disjunction in mice (Stemmann et al., 2001; Hagting et al., 2002; Chang et al., 2003; Herbert et al., 2003). To analyze whether the degradation of cyclin B1 (CYB-1), was normal in *cul-2(RNAi)* embryos, we used the *pie-1* promoter to express CYB-1::GFP in the germline. In wild type, CYB-1::GFP fluorescence was detected in mature oocytes, but rapidly disappeared during meiosis I and II following fertilization (Fig. 3A,B). By contrast, in *cul-2(RNAi)* embryos, CYB-1::GFP signal decreased only modestly during meiosis and remained at elevated levels in mitotic-stage embryos (Fig. 3A,B). Elevated levels of CYB-1 were also detected in *cul-2(RNAi)* embryos with an anti-CYB-1 antibody kindly provided by Sander van den Heuvel (MGH Cancer Center, USA) (data not shown). A similar defect in CYB-1::GFP degradation was observed in *zyg-11(RNAi)* embryos (Fig. 3A).

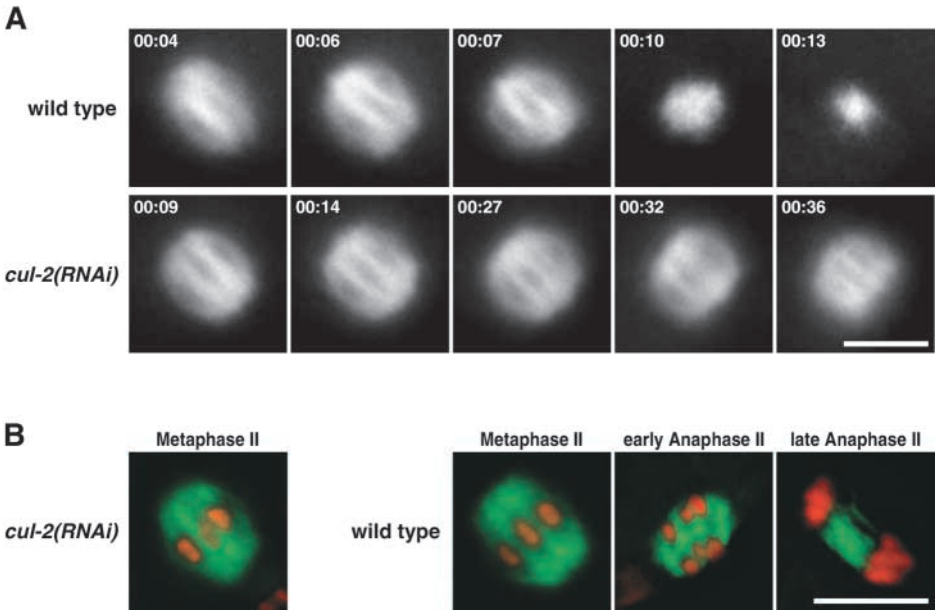

Fig. 4. The meiosis II spindle in *cul-2(RNAi)* zygotes maintains a normal morphology for an extended period. (A) β-tubulin::GFP epifluorescence movie sequences of live wild-type (upper) and *cul-2(RNAi)* (lower) zygotes to show meiotic II spindle dynamics. Time post-anaphase I is indicated in the upper left corner of images (hours:minutes). (B) Overlaid epifluorescence images of anti-α-tubulin (green) and DAPI (red) staining of meiosis II spindles for wild type (right) and *cul-2(RNAi)* (left) zygotes. The stage of meiosis is indicated above the image. Scale bars: 5 μm.

Given the requirement for cyclin B1 degradation for entry into anaphase in mammals, we tested whether the failure to degrade cyclin B1 was responsible for the *cul-2* metaphase II arrest phenotype. RNAi depletion of *cyb-1* does not affect the timing of meiosis II (Fig. 3C). If the elevated level of CYB-1 in *cul-2* mutants was solely responsible for the metaphase arrest then depletion of CYB-1 would be expected to allow *cul-2* mutants to proceed through anaphase. However, this is not the case, as chromosome segregation was not observed in six out of 12 of the *cul-2(ek1); cyb-1(RNAi)* embryos, a ratio similar to that observed in *cul-2* mutants alone. Interestingly, in *cul-2(ek1)* homozygous embryos depleted for *cyb-1*, chromosomes were observed to split in three directions at anaphase I in three out of 12 embryos, and in all 12 embryos examined, chromosomes did not form a pentagonal array in meiosis II (data not shown). This latter result is surprising as pentagonal arrays form in both *cyb-1(RNAi)* and *cul-2(ek1)* homozygous meiosis II-stage embryos (Fig. 1A; data not shown). Although the anaphase defect was not rescued, *cyb-1* RNAi did produce a partial rescue of the *cul-2* meiotic delay phenotype. In seven out of 12 *cul-2(ek1); cyb-1(RNAi)* embryos, meiosis II length was similar to that in *cul-2(ek1)* embryos; however, the remaining five embryos had significantly shorter meiosis II timings, three of which were indistinguishable from wild type (Fig. 3C).

The anaphase-promoting complex/cyclosome (APC/C) ubiquitin ligase promotes cyclin B degradation during mitosis in yeast and metazoa (Peters, 2002). APC/C also promotes cyclin B degradation during meiosis in *Xenopus* and mouse (Peter et al., 2001, Nixon et al., 2002). In *C. elegans*, loss of APC/C produces a one-cell embryonic arrest at metaphase of meiosis I (Furuta et al., 2000; Davis et al., 2002). Levels of CYB-1::GFP were stabilized in *apc-11(RNAi)* embryos (Fig. 3B), suggesting that both CUL-2 and APC/C are required for CYB-1 degradation.

The meiotic spindle maintains normal morphology for an extended period in *cul-2(RNAi)* zygotes

We studied the morphology and dynamics of the meiotic spindle in *cul-2(RNAi)* zygotes by both anti-α-tubulin antibody staining and live β-tubulin::GFP movies. In meiosis I, the meiotic spindles of *cul-2(RNAi)* and wild-type embryos were indistinguishable (data not shown). Meiosis II spindles in *cul-2(RNAi)* embryos maintained a normal barrel-shaped structure for an extended period of time (Fig. 4A). Eventually, the *cul-2(RNAi)* meiotic spindle shrunk and lost its barrel structure. On average, the *cul-2(RNAi)* meiosis II spindle lasted three times as long as in wild type (36.2±2.5 versus 12.2±0.7 minutes, n=6 for each) (Fig. 4A). Meiotic spindle morphology characteristic of anaphase II (Fig. 4B) was never observed in *cul-2(RNAi)* embryos.

Perdurance of the Meiosis II spindle is associated with polarity reversal

In wild-type embryos after meiosis, PAR-3 and PAR-6 are expelled from the posterior cortex near the sperm asters, and, concomitantly, PAR-2 stably accumulates on the posterior cortex (Hung and Kemphues, 1999; Boyd et al., 1996) (Fig. 5A). In contrast to wild type, *cul-2(RNAi)* zygotes stably accumulate cortical PAR-2 while still in meiosis II. We analyzed the PAR-2 localization pattern in meiosis II-stage *cul-2(RNAi)* zygotes using immunofluorescence with anti-PAR-2 antibodies. In the majority of meiosis II-stage *cul-2(RNAi)* embryos (76%, 50/67), strong cortical PAR-2 staining was observed on the anterior cortex, a reversal of the wild-type pattern (Fig. 5A; Table 1). *zyg-11(RNAi)* embryos similarly had a high percentage of anterior-localized PAR-2 (Fig. 5C; Table 1). PAR-3 and PAR-6 localizations were also reversed, with exclusion of both proteins from the anterior cortex in the majority of *cul-2(RNAi)* embryos (23/33 and 8/10, respectively; Fig. 5A).

We analyzed whether downstream aspects of polarity were reversed in *cul-2(RNAi)* embryos. After meiosis is completed in wild type, dispersed P granules move toward the posterior and are completely in the posterior half by the pronuclei meeting stage (Strome and Wood, 1983) (Fig. 5D). In *cul-2(RNAi)* zygotes, P granules can localize to the anterior, posterior, center or lateral cytoplasm. The abnormal localization is coupled to the altered placement of PAR-2, as P granules co-localize with anterior or lateral cortical PAR-2 in the majority of mitotic *cul-2(RNAi)* embryos (10/11; Fig. 5D).

In wild type, maternal pronuclei migrate from the anterior to meet the sperm pronucleus in the posterior (Fig. 5E). This

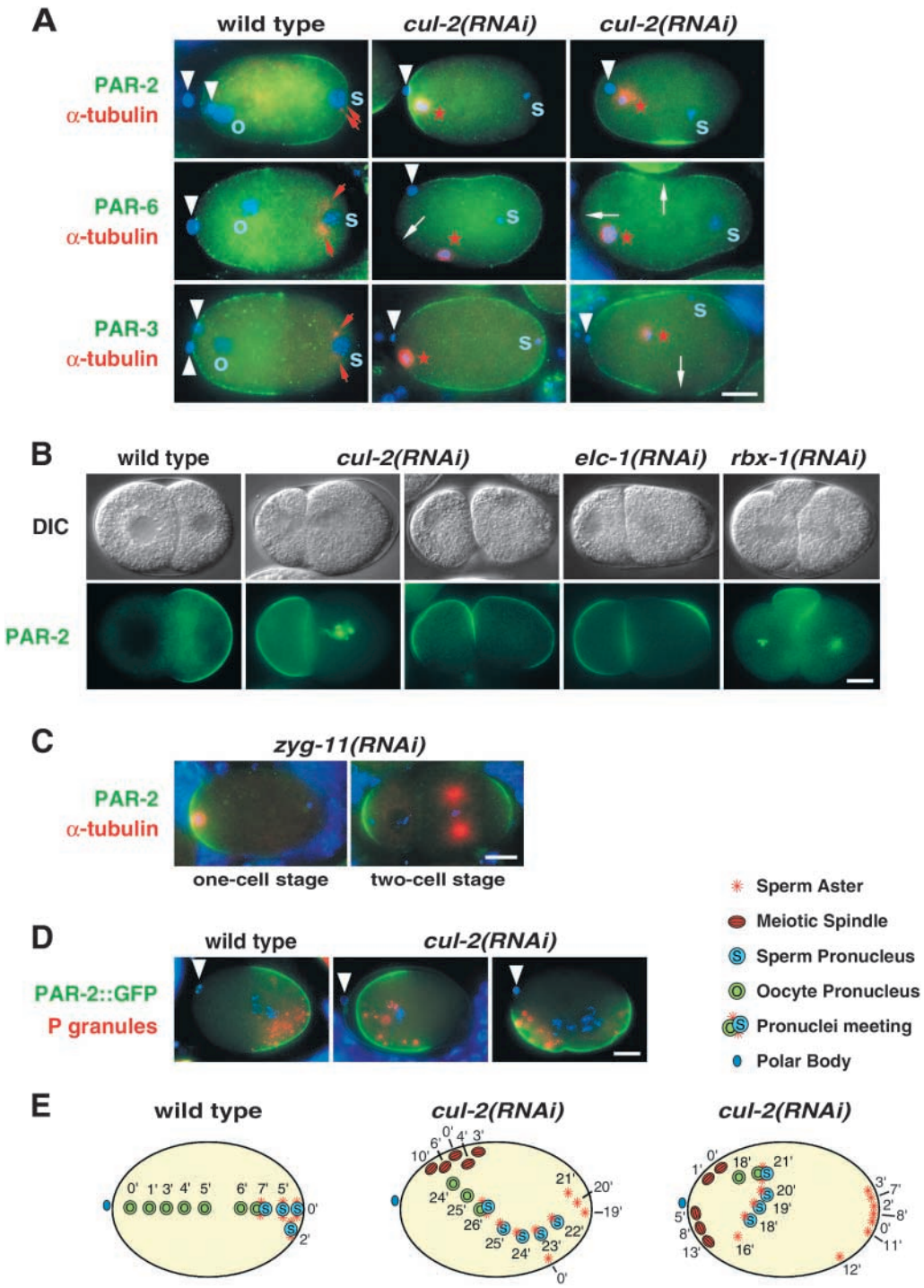

Fig. 5. Polarity defects in *cul-2*, *elc-1*, *rbx-1* and *zyg-11* RNAi embryos. (A) Overlaid epifluorescence images of anti-PAR-2 (green, upper panel), anti-PAR-6 (green, middle panel), anti-PAR-3 (green, lower panel), anti-α-tubulin (red), and DAPI (blue) staining in wild-type (left) and *cul-2(RNAi)* (middle and right) zygotes. The wild-type zygotes are in interphase, whereas the *cul-2(RNAi)* zygotes are in meiosis II. Red stars denote meiotic spindles; red arrows, sperm asters; o, maternal pronuclei; s, sperm DNA; white arrowheads, polar bodies; and white arrows, regions of the cortex lacking PAR-6 or PAR-3 staining. (B) Matched DIC and PAR-2::GFP images of two-cell stage wild-type, *cul-2(RNAi)*, *elc-1(RNAi)* and *rbx-1(RNAi)* embryos. (C) Overlaid epifluorescence images of anti-PAR-2 (green), anti-α-tubulin (red) and DAPI (blue) staining in *zyg-11(RNAi)* one-cell (left) and two-cell (right) stage embryos. (D) P granule localization in mitotic *cul-2(RNAi)* embryos: PAR-2::GFP (green), anti-P granule (red) and DAPI (blue). White arrowheads denote polar bodies. (E) Diagram of migration of spindles and pronuclei in wild-type (left) and *cul-2(RNAi)* zygotes (middle and right) derived from β-tubulin::GFP/DIC movies. Timing begins with the initial observation of sperm asters and ends at pronuclei meeting. In five out of five *cul-2(RNAi)* embryos, the sperm asters formed during meiosis, although they were very small relative to their size after meiosis. Anterior is to the left. Scale bars: 10 μm.

aspect of polarity is also reversed in *cul-2(RNAi)* embryos. In the majority of *cul-2(RNAi)* embryos (8/10), the sperm pronucleus migrates further than the maternal pronucleus (Fig. 5E). Pronuclei often meet in the anterior of the embryo rather than in the posterior, and the anterior daughter cell is smaller than the posterior cell in over half of *cul-2(RNAi)* embryos (16/31; Fig. 5B). Similar polarity defects were observed in *elc-1* and *rbx-1* RNAi embryos (Fig. 5B; data not shown).

To study whether the polarity reversal correlated with the extended meiosis II delay in *cul-2(RNAi)* zygotes, we varied the penetrance of *cul-2* RNAi depletion by altering the length of time adult hermaphrodites were exposed to *cul-2* dsRNA prior to fertilization. The partial *cul-2* RNAi treatment produced meiosis II timing ranging from that of wild type to delays similar to that of *cul-2(ek1)* null mutants (Table 2). In wild type, meiosis II lasted 16.2±1.3 minutes and PAR-2::GFP accumulated on the posterior cortex approximately 2 minutes after the completion of meiosis II (18.4±0.9 minutes after meiosis I; Table 2). In two of five wild-type zygotes, transient, weak, anterior cortical PAR-2::GFP was observed during

Table 1. PAR-2 localization in *cul-2*, *zyg-11* and *tbb-2* RNAi embryos

		PAR-2 localization in meiosis II embryos (%)					
Condition	*n*	Anterior	Lateral*	Circular*	Faint all around	None	Posterior
cul-2(RNAi); PAR-2 antibody	67	76.1	12.1 (7.5)	0	0	9.0	3.0
zyg-11(RNAi); PAR-2 antibody	58	69.0	3.4 (0)	0	3.4	19.0	5.2
cul-2(RNAi); PAR-2::GFP	54	44.4	13.0 (3.7)	29.6 (9.3)	13	0	0
zyg-11(RNAi); PAR-2::GFP	47	59.6	6.4 (0)	12.8 (0)	21.3	0	0
tbb-2; cul-2 RNAi; PAR-2::GFP†	36	0‡	5.6 (5.6)	2.8 (0)	13.9	77.8	2.8‡
tbb-2(RNAi); PAR-2::GFP†	11	0	0	0	0	100	0
PAR-2::GFP	13	7.7 (faint)	0	0	23.1	69.2	0

*Numbers in parentheses denote the percentage of embryos in which the lateral or circular PAR-2 is distant from the meiotic spindle.
†*tbb-2(RNAi)* embryos do not undergo meiosis I, so *tbb-2(RNAi)* numbers represent all embryos in meiosis, rather than just meiosis II embryos.
‡One *cul-2* RNAi; PAR-2::GFP embryo had an ambiguous localization with both meiotic DNA and condensed sperm DNA in the same end with cortical PAR-2::GFP (see Fig. 6E, right). We have assigned the localization to the posterior because the sperm DNA generally remains in one end of the embryo in *tbb-2(RNAi)* embryos while the meiotic DNA location is much more variable.

Table 2. Cortical PAR-2 localization and division pattern upon titration of *cul-2* RNAi

Genotype/treatment	Meiosis II duration (minutes)	Initiation of anterior or lateral PAR-2 (minutes after start of meiosis II)	Initiation of posterior PAR-2 (minutes)	Cell size in two-cell stage embryo	PAR-2 localization in two-cell stage
Wild type	17	–	19	AB>P_1	P_1
Wild type	14	–	19	AB>P_1	P_1
Wild type	16	3 Transient, weak anterior†	19	AB>P_1	P_1
Wild type	17	–	17	AB>P_1	P_1
Wild type	17	11 Transient, weak anterior†	18	AB>P_1	P_1
cul-2(RNAi)	16	9 Transient, weak anterior†	20	AB>P_1	P_1
cul-2(RNAi)	16	–	21	AB>P_1	P_1
cul-2(RNAi)	17	–	18	AB>P_1	P_1
cul-2(RNAi)	23	11 Transient, weak anterior†	19	AB>P_1	P_1
cul-2(RNAi)	28	12 Anterior	44	AB>P_1	P_1
cul-2(RNAi)	30	16 Anterior	28	AB>P_1	AB and P_1
cul-2(RNAi)	32	16 Lateral*	35	AB>P_1	P_1
cul-2(RNAi)	37	24 Lateral*	49	AB>P_1	AB and P_1
cul-2(RNAi)	42	29 Anterior	58	AB>P_1	AB and P_1
cul-2(RNAi)	42	21 Lateral*	–	AB=P_1	AB and P_1
cul-2(RNAi)	48	16 Anterior	–	AB<P_1	AB
cul-2(RNAi)	51	33 Anterior	–	AB<P_1	AB

These experiments were performed with a wild-type strain expressing PAR-2::GFP and β-tubulin::GFP (JH1473). All times are from the end of meiotic anaphase I. No occurrence is denoted by a dash (–).
*Lateral PAR-2 patches arose distant from the meiotic spindle.
†Transient and weak anterior PAR-2 patches were of lower intensity than the general interior cytoplasmic PAR-2::GFP signal.

meiosis II, similar to previous reports (Boyd et al., 1996; Cuenca et al., 2003) (Table 2). Transient, weak, anterior PAR-2 localizations were also observed in two *cul-2(RNAi)* embryos that had meiosis II timing similar to wild type (Table 2). *cul-2(RNAi)* zygotes with meiosis II timing of ⩾28 minutes developed intense, stable PAR-2::GFP patches on anterior or lateral cortexes (Table 2). An extended meiotic delay coupled with an anterior PAR-2::GFP patch was associated with a reversal in the longitudinal placement of the mitotic spindle, so that the first division produced a posterior cell larger than the anterior cell (Table 2).

Ectopic lateral PAR-2 localization is associated with loss of CUL-2

We were intrigued by the observation in *cul-2(RNAi)* zygotes of PAR-2 patches (8/67 embryos), and exclusions of PAR-3 (3/33) and PAR-6 (2/10), on the lateral cortex that were often distant from both the meiotic spindle and the SPCC (Fig. 5A; Table 1). As microtubule (MT) organizing foci have been implicated in PAR-2 localization (O'Connell et al., 2000; Wallenfang and Seydoux, 2000), we sought to determine whether the lateral PAR-2 arose from prior transient association of the meiotic spindle or SPCC with the lateral cortex. To address this, we followed the initiation of cortical PAR-2 in living embryos expressing either a combination of PAR-2::GFP and β-tubulin::GFP (to visualize the meiotic spindle), or PAR-2::GFP and histone H2B::GFP (to visualize oocyte and sperm DNA). In the two strains, PAR-2 patches appeared to initiate distant from the meiotic spindle or distant from both oocyte and sperm DNA (5/20 and 3/10 embryos, respectively) (Fig. 6A). With the PAR-2::GFP strains, we observed a higher percentage of lateral accumulation of PAR-2 upon *cul-2* RNAi than was observed for *cul-2(RNAi)* embryos probed with anti-PAR-2 antibodies (Table 1). In particular, we observed a substantial percentage of embryos in which PAR-2::GFP spread extensively on the cortex to form a circular band around the embryo (Fig. 6B; Table 1). One third of the circular PAR-2 patterns were observed distant from the

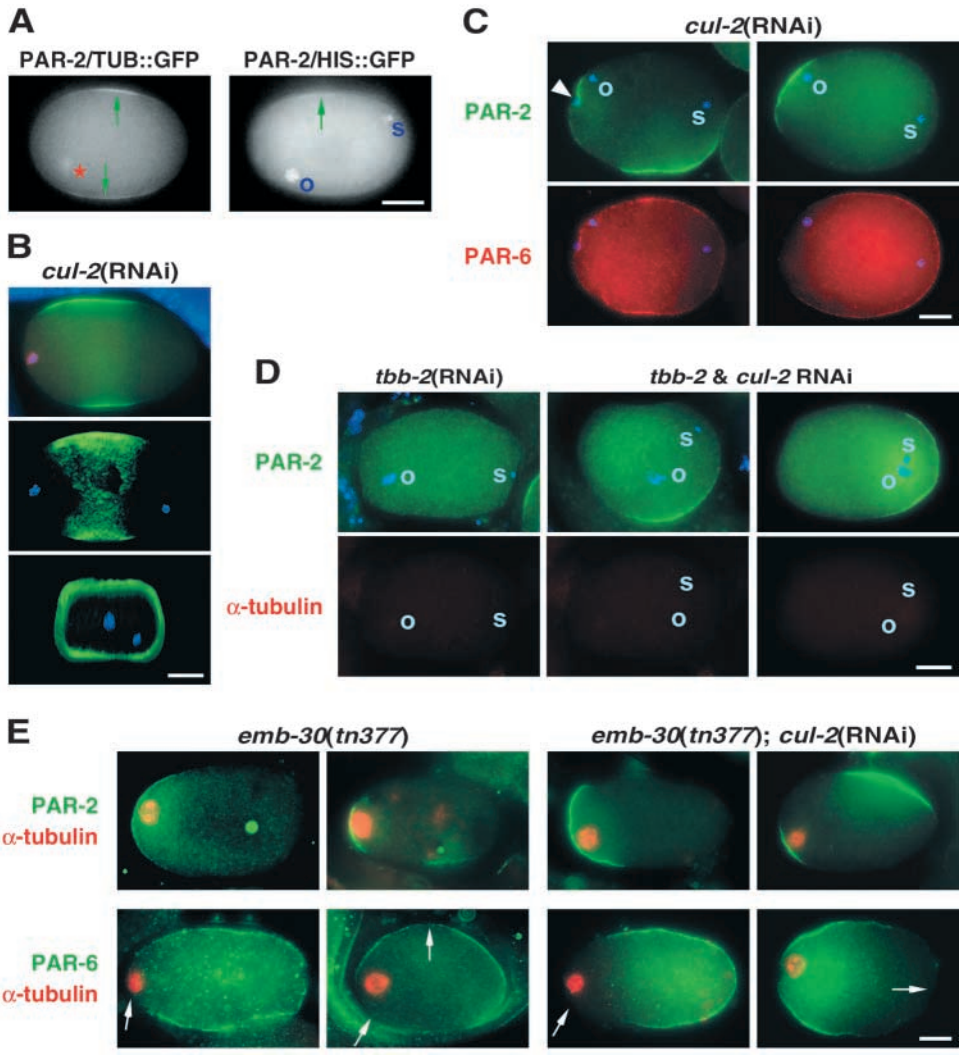

Fig. 6. Ectopic lateral PAR-2 in *cul-2(RNAi)* embryos. (A) The initial localization of lateral PAR-2, as monitored in epifluorescence movies of *cul-2(RNAi)* embryos expressing PAR-2::GFP and β-tubulin::GFP (left), and PAR-2::GFP and histone H2B::GFP (right). Green arrows denote cortical PAR-2. Cortical PAR-2::GFP signals were observed in regions that were distal to the meiotic spindle (left), or to oocyte and sperm DNA (right), during the entire time period post-fertilization. (B) Epifluorescence (top) and confocal three-dimensional reconstruction of a *cul-2(RNAi)* embryo showing a circular PAR-2 pattern: PAR-2::GFP (green), anti-α-tubulin (red) and DAPI (blue). Note that the confocal reconstruction is only of the embryo and excludes the surrounding germ cell DAPI signal. Middle image shows a side view; bottom image, anterior is to the front. (C) Simultaneous localization of PAR-2 and PAR-6 in meiosis II-stage *cul-2(RNAi)* embryos. (Left) Anterior and lateral PAR-2::GFP (top) with uniform anti-PAR-6 staining (bottom). (Right) Anterior anti-PAR-2 staining with anterior exclusion of PAR-6::GFP. (D) PAR-2::GFP localization in *tbb-2(RNAi)* and *tbb-2; cul-2* double RNAi meiotic embryos. Epifluorescence images of PAR-2::GFP (green, top), DAPI (blue, top) and anti-α-tubulin (red, bottom). o, location of maternal DNA; s, location of sperm DNA. The left *tbb-2; cul-2* double RNAi embryo has a lateral PAR-2::GFP patch, whereas the right embryo has PAR-2::GFP on the end of the embryo near both the maternal and condensed sperm DNA. (E) *emb-30(tn377)* (left) and *emb-30(tn377); cul-2(RNAi)* (right) zygotes were stained with anti-α-tubulin (red) and either anti-PAR-2 (green, upper panel) or anti-PAR-6 (green, lower panel). For each genotype, left panels show anterior PAR-2 localization (top) or PAR-6 exclusion (bottom), and right panels show lateral/posterior PAR-2 localization (top) or PAR-6 exclusion (bottom). White arrows denote regions of the cortex lacking PAR-6 staining. Anterior is to the left. Scale bars: 10 μm.

meiotic spindle (Fig. 6B; Table 1). These observations of PAR-2 accumulation distant from the meiotic spindle suggest that in *cul-2(RNAi)* embryos, the initiation or spreading of cortical PAR-2 is under less stringent control.

In wild-type zygotes, PAR-2 and PAR-6 cortical localizations are mutually antagonistic (Watts et al., 1996; Hung and Kemphues, 1999; Cuenca et al., 2003). It has been proposed that the normal accumulation of PAR-2 on the posterior cortex occurs after the exclusion of PAR-6 (Cuenca et al., 2003). With a combination of anti-PAR-6 antibodies and PAR-2::GFP, we observed that ten out of twelve lateral or circular PAR-2 patches that were distant from the meiotic spindle had overlapping cortical PAR-6, suggesting that the lateral PAR-2 localization can occur without the prior removal of PAR-6 (Fig. 6C).

Interestingly, the percentage of lateral and circular PAR-2 was significantly lower in *zyg-11(RNAi)* embryos, with no examples of PAR-2 patches distant from the meiotic spindle observed (Table 1). Although this may reflect a reduced effectiveness of the RNAi procedure in depleting ZYG-11 relative to CUL-2, it nevertheless suggests that the lateral accumulation of PAR-2 does not arise directly from the meiotic delay, as RNAi of both genes gave comparable meiotic lengths but only *cul-2(RNAi)* embryos had lateral patches distant from the meiotic spindle.

To further test whether the accumulation of PAR-2 distant from the meiotic spindle was a secondary consequence of the meiotic delay or reflected the loss of a separable CUL-2 function, we analyzed PAR-2 localization in an *emb-30* mutant background. *emb-30* encodes the APC/C component APC-4 (Furuta et al., 2000). At the restrictive temperature of 24°C, *emb-30(tn377*ts*)* embryos arrest at the metaphase I stage of meiosis (Furuta et al., 2000). As described above, CUL-2 is not required for progression through meiosis I; *emb-30(tn377); cul-2(RNAi)* embryos have the same metaphase I-arrest phenotype and spindle morphology as *emb-30(tn377)* embryos (Fig. 6E; data not shown). Therefore, any differences in PAR-2 localization between the two strains should reflect the loss of

CUL-2 functions that are independent of its role in meiotic progression. As expected from previous work on *emb-30* by Wallenfang and Seydoux (Wallenfang and Seydoux, 2000), we observed that a high percentage of both *emb-30(tn377)* and *emb-30(tn377); cul-2(RNAi*) embryos had anterior PAR-2 (89%, *n*=54, and 83%, *n*=47, respectively). In *emb-30(tn377)* zygotes, only a small minority of embryos had lateral or posterior PAR-2 patches (3.7%, 2/54) (Fig. 6E), as was also observed by Wallenfang and Seydoux (Wallenfang and Seydoux, 2000). In *emb-30(tn377); cul-2(RNAi*) zygotes, however, the percentage of embryos with lateral or posterior PAR-2 patches was significantly higher (23%, 11/47; $P<0.01$); most of these embryos also had anterior PAR-2 patches (Fig. 6E). Similarly, 27% of *emb-30(tn377); cul-2(RNAi*) zygotes (*n*=56) exhibited an exclusion of PAR-6 on lateral or posterior cortexes compared with 4% of *emb-30(tn377)* zygotes (*n*=28) (significance of $P<0.05$) (Fig. 6E). There was no difference in the MT distributions observed in *emb-30(tn377)* and *emb-30(tn377); cul-2(RNAi)* embryos, both of which had disorganized spindles at comparable percentages (43% and 33%, respectively). These results provide evidence that CUL-2 has a separable function to prevent the ectopic initiation or spreading of cortical PAR-2.

Our observations suggested that the lateral PAR-2 patches could occur distant from the meiotic spindle or sperm DNA. To rigorously test whether PAR-2 can localize to the cortex in the absence of the meiotic spindle in *cul-2(RNAi)* embryos, we disrupted MTs by depleting the β-tubulin gene *tbb-2*, which had the effect of eliminating the meiotic spindle and visible MTs during meiosis. The elimination of MTs made distinguishing the two meiotic stages problematic because of the loss of chromosome and spindle dynamics. Therefore, all meiotic embryos were analyzed rather than just those in meiosis II, the stage in which ectopic PAR-2 localization generally occurs. We observed that in *tbb-2*; *cul-2* double RNAi embryos, the overall percentage of cortical PAR-2 was markedly reduced, particularly in the anterior where PAR-2 is normally associated with the meiotic spindle (Table 1). However, discrete PAR-2 patches were still observed in 11.2% of meiotic embryos, most of which was localized to the lateral cortex (Fig. 6D; Table 1). Wild-type embryos subjected to *tbb-2* RNAi had no meiotic PAR-2 staining (Table 1). These results indicate that PAR-2 localization can occur in *cul-2(RNAi)* embryos in the absence of the meiotic spindle. However, the reduction in the percentage of lateral PAR-2 localization in *tbb-2*; *cul-2* RNAi embryos relative to *cul-2(RNAi)* embryos suggests that the presence of MTs potentiates the ectopic PAR-2 localization.

Interestingly, depletion of *tbb-2* alone produced a high percentage of post-meiotic embryos with condensed mitotic prometaphase chromosomes and cortical PAR-2 localized in the same half of the embryo. In 13 out of 15 of these embryos, α-tubulin staining was observed in one or two small circles of approximately 0.3 μm diameter near the condensed chromosomes, presumably the centrosomes. For *tbb-2, cul-2* RNAi embryos with mitotic prometaphase chromosomes, 8 out of 12 had one or two similar small α-tubulin circles, with PAR-2 either localized on the cortical half of the embryo with the chromosomes and α-tubulin circles (9/12) or on lateral cortexes distant from α-tubulin circles (3/12). The observation of α-tubulin at the centrosome suggests that even though visible MT filaments were eliminated after *tbb-2* RNAi, a residual capacity for tubulin to be organized into the centrosome still exists and potentially this structure is capable of localizing PAR-2. Therefore, although our results demonstrate that the loss of CUL-2 during meiosis can localize cortical PAR-2 in the absence of the meiotic spindle, we cannot conclude that the PAR-2 localization is independent of all MT activity.

Discussion

CUL-2 and ZYG-11 are required for the initiation of anaphase II and meiotic progression

In zygotes devoid of CUL-2, anaphase II either fails to occur or is severely delayed, and meiosis II lasts three to four times longer than in wild type. The delay in meiotic exit may be more than just a secondary effect of the failure of anaphase II, as *air-2(RNAi)* and *rec-8(RNAi)* zygotes have normal meiotic timing even though the former lacks anaphase I and II, and the latter lacks anaphase II (Rogers et al., 2002) (this study).

Three lines of evidence indicate that the meiosis II defects in *cul-2* mutants do not arise from a failure of chromosome separation. First, the cohesin REC-8, which is required to hold sister chromatids together (Pasierbek et al., 2001), dissociates from metaphase II chromosomes in *cul-2* mutants. Second, a small percentage of *cul-2* mutant zygotes are observed in which sister chromatids separate during meiosis II but still fail to move to the spindle poles. And third, in *cul-2(RNAi); rec-8(RNAi)* zygotes, all chromatids separate from each other, yet exit from meiosis II is still delayed.

Mitotic anaphase chromosome movement has been extensively analyzed. Both MT spindle dynamics and MT motors are required for mitotic anaphase poleward force generation (Wittmann et al., 2001). By contrast, meiotic anaphase has not been extensively studied, and it is unclear to what extent similar mechanisms will function to move chromosomes during meiosis. Interestingly, the morphology and dynamics of the *C. elegans* meiotic spindle are quite different from the mitotic spindle. The mitotic spindle is composed of long polar MTs and relatively short midzone MTs. Ablation of the mitotic midzone MTs increases the velocity and distance of chromosome separation, suggesting that they are not required to ‘push’ chromosomes apart but instead function to limit the speed and/or extent of chromosome movement (Grill et al., 2001). By contrast, during meiotic anaphase, the MTs near the meiotic spindle poles appear to depolymerize, whereas the amount of midzone MTs between the separating chromosomes increases dramatically (Albertson and Thomson, 1993) (Fig. 4B). During late anaphase, all MTs appear to be located between the separating chromosomes (Fig. 4B). The reorganization of MTs to the midzone that occurs during meiotic anaphase suggests that meiotic chromosomes are ‘pushed’ apart by MT polymerization between the chromosomes rather than being ‘pulled’ to the spindle poles as occurs during mitosis. In *cul-2* mutants, the meiotic spindle maintains its normal size and shape for an extended period of time during metaphase II, indicating a defect in the initiation of MT depolymerization at the spindle poles and polymerization between sister chromatids. CUL-2 therefore appears to function upstream of

the dramatic MT rearrangements that occur during meiotic chromatid segregation.

CUL-2 and ZYG-11 are required for the degradation of Cyclin B1 during meiosis

Using a CYB-1::GFP reporter, we observed that maternally-provided cyclin B1 is degraded upon fertilization. In both *cul-2(RNAi)* and *zyg-11(RNAi)* embryos, CYB-1::GFP is stabilized during both meiosis I and II. This is not a secondary consequence of the meiosis II arrest, as the failure to degrade CYB-1::GFP precedes the arrest. Surprisingly, depletion of CYB-1 by RNAi in *cul-2(ek1)* mutants produced a synthetic phenotype of loss of the pentagonal chromosome array in meiosis II, indicating that *cul-2* mutant zygotes have additional meiotic defect(s) that are exacerbated by loss of CYB-1. The depletion of CYB-1 partially rescued the meiosis II delay of *cul-2(ek1)* embryos, suggesting that the failure to degrade CYB-1 may be contributing to the meiotic delay.

The APC/C ubiquitin ligase promotes cyclin B degradation during mitosis in yeast and metazoa (Peters, 2002). APC/C has also been shown to promote meiotic cyclin B degradation in budding yeast, fission yeast, *Xenopus* and mouse (Cooper et al., 2000; Blanco et al., 2001; Peter et al., 2001; Nixon et al., 2002). In *C. elegans*, inactivation of the APC component *apc-11* also stabilized cyclin B1 levels. Further research will be required to assess the roles of CUL-2 and APC/C in regulating cyclin B1 levels.

The spindle dynamics of anaphase I and II appear to be similar to each other in wild type (Albertson and Thomson, 1993). Therefore it is surprising that in *cul-2(ek1)* embryos, anaphase I is normal but anaphase II is severely delayed or abolished. This is not due to the perdurance of *cul-2* maternal product through meiosis I because these embryos arose from *cul-2(ek1)* homozygous hermaphrodite parents; furthermore, *cul-2(ek1)* embryos completely lack anti-CUL-2 staining (Feng et al., 1999). The initiation of the metaphase to anaphase transition in the two meiotic stages therefore appears to be differentially regulated.

CUL-2 ubiquitin ligase complex components share meiotic and polarity functions

In mammals, elongin C has been shown to interact with CUL2 and CUL5, but not with other cullins (Pause et al., 1999; Kamura et al., 2001). CUL2 and CUL5 share homology in the N-terminal region, which is required for elongin C binding (Pause et al., 1999; Pintard et al., 2003b). Inactivation of CUL-5 in *C. elegans* does not produce visible phenotypes (Kamath et al., 2003), suggesting that it is not involved in the meiotic or polarity defects described in this work. RNAi depletion of *elc-1* phenocopies all visible *cul-2* mutant phenotypes, including the G1 arrest of germ cells (Hui Feng and E.T.K., unpublished), as well as the degradation of embryonic CCCH proteins (DeRenzo et al., 2003), suggesting that ELC-1 participates in all known CUL-2 functions. RBX-1 depletion in *C. elegans* phenocopies multiple cullin loss-of-function phenotypes (Sasagawa et al., 2003) (data not shown), consistent with its interaction with multiple cullins in mammals (Ohta et al., 1999). The observation of meiotic and polarity defects upon inactivation of homologs of both core CUL-2 complex components suggests that CUL-2 functions in the context of a conserved ubiquitin ligase complex.

A substrate recognition component (SRC) is required for the core CUL-2 complex to bind substrates. A number of mammalian CUL2 SRCs have been identified that function in distinct CUL2 E3 complexes, including the von Hippel-Lindau tumor suppressor protein (VHL) (Kim and Kaelin, 2003; Kamizono et al., 2001; Brower et al., 2002). Inactivation of the *C. elegans* VHL ortholog produces no embryonic phenotypes (Epstein et al., 2001), indicating that SRCs other than VHL are required for the CUL-2 meiotic and embryonic functions.

Currently, the only genes in *C. elegans* known to specifically affect the meiosis II metaphase-to-anaphase transition are CUL-2 complex components and *zyg-11*. Combining homozygous null alleles of both *cul-2* and *zyg-11* in the same embryo did not enhance the meiotic phenotype, which is consistent with both genes functioning in the same pathway. Both genes also share other embryonic phenotypes, including multiple nuclei, cytoplasmic extensions, and embryonic arrest with approximately 24 cells (Kemphues et al., 1986; Feng et al., 1999) (data not shown). ZYG-11 is a leucine-rich repeat protein and this protein-interaction motif is found in a number of SRCs for CUL-1-based SCF E3 complexes (Tyers and Jorgensen, 2000). It is therefore possible that ZYG-11 functions as an SRC in one of the CUL-2-based E3 complexes to promote meiosis; although our data suggests that ZYG-11 does not function with CUL-2 to promote germ cell proliferation. As the localization of PAR-2 independently of MT-foci was not observed in *zyg-11(RNAi)* embryos, currently there is no evidence that ZYG-11 functions to restrain PAR-2 localization in regions distant from MT-organizing centers.

Meiotic timing and AP polarity

During the extended meiosis II in *cul-2* mutants, the majority of embryos accumulate stable PAR-2 on the anterior cortex near the meiotic spindle. It has been shown that in APC/C mutant zygotes arrested in meiosis I, the meiotic spindle can initiate the localization of PAR-2 onto the anterior cortex (Wallenfang and Seydoux, 2000). The disorganized ‘frayed’ appearance of the meiotic spindle observed in older meiosis I-arrested embryos was proposed to initiate the PAR-2 reversal (Wallenfang and Seydoux, 2000). By contrast, our study found that stable anterior PAR-2 localizations occur with meiosis II spindles of normal morphology and with timing similar to the appearance of PAR-2 on the posterior cortex in wild type. In addition, we observed that P granules segregate toward the mislocalized PAR-2, that the SPCC migrates further than the meiotic pronucleus, and that the cell division plane is often asymmetrically positioned to produce a reversal in daughter cell size. None of these downstream polarity changes are observed in meiosis I-arrested APC/C mutants (Wallenfang and Seydoux, 2000), suggesting either that the meiosis II spindle is fundamentally different than the meiosis I spindle in effecting polarity or that these changes can only manifest upon entry into interphase.

Transient and weak PAR-2 patches occasionally arise on the anterior cortex during meiosis II in wild-type zygotes, which suggests that the intact meiosis II spindle has an intrinsic ability to direct PAR-2 localization (Table 2) (Boyd et al., 1996; Cuenca et al., 2003). We observed that the longer *cul-2(RNAi)* zygotes remained in meiosis, the more stabilized the anterior PAR-2 became and the less likely that a posterior PAR-2 patch would form. With only a modest meiosis II delay, a full reversal

of PAR localization was observed, with PAR-2 exclusively on the anterior and the asymmetric cleavage of the zygote reversed (Table 2). The failure of PAR-2 to localize to the posterior in these *cul-2(RNAi)* embryos may derive in part from the aberrant migration of the SPCC to the anterior, which begins during meiosis (Fig. 5E). In *cul-2(RNAi)* embryos, sperm asters generally form during meiosis but are very small until meiosis is completed, presumably because of the effect of the MT-severing katanin MEI-1, which is degraded after meiosis (Pintard et al., 2003a). Therefore, the failure of the SPCC to form full mitotic asters while in the posterior may contribute to the lack of PAR-2 in that region. In total, our results suggest that only a short window of meiotic timing is compatible with the proper placement of the AP axis.

CUL-2 limits the inappropriate localization of PAR-2

The establishment of AP polarity in the *C. elegans* zygote has been proposed to be a MT-directed process (O'Connell et al., 2000; Wallenfang and Seydoux, 2000). In *cul-2(RNAi)* embryos, PAR-2 was observed to initiate cortical localization distant from the meiotic spindle or sperm DNA. Upon elimination of the meiotic spindle by RNAi depletion of the β-tubulin TBB-2, lateral cortical PAR-2 was still observed in *cul-2(RNAi)* embryos at significant although somewhat reduced levels. This suggests that the aberrant PAR-2 localization is not dependent on the presence of a MT organizing center, although MTs may potentiate the localization. The ectopic PAR-2 localization in *cul-2* mutants does not appear to arise as a secondary consequence of the meiosis II delay, as the depletion of CUL-2 produces a significant increase in ectopic PAR-2 localization even in an *emb-30* mutant background in which embryos are arrested in metaphase I. Furthermore, although ZYG-11 is also required for meiotic progression, the localization of PAR-2 distant from the meiotic spindle was not observed in *zyg-11(RNAi)* embryos. We propose that CUL-2 has a separate function to restrain ectopic PAR-2 association with the cortex during meiosis. In combination with the recently described role for CUL-2 in degrading germ cell determinants in anterior cells of the early embryo (DeRenzo et al., 2003), our results indicate that CUL-2 promotes the initiation of AP polarity through multiple mechanisms.

We thank Yuji Kohara for cDNA clones; the *Caenorhabditis* Genetics Center for strains; Hui Feng, Vikas Dhingra, Kenneth Kemphues, Josef Loidl, Susan Strome, Geraldine Seydoux and Sander van den Heuvel for reagents; and Sander van den Heuvel for comments on the manuscript. This work was supported by a grant from the American Cancer Society (RSG-01-251-01-DDC) to E.T.K.

References

Albertson, D. G. and Thomson, J. N. (1993). Segregation of holocentric chromosomes at meiosis in the nematode, *Caenorhabditis elegans*. *Chromosome Res.* **1**, 15-26.

Blanco, M. A., Pelloquin, L. and Moreno, S. (2001). Fission yeast mfr1 activates APC and coordinates meiotic nuclear division with sporulation. *J. Cell Sci.* **114**, 2135-2143.

Boyd, L., Guo, S., Levitan, D., Stinchcomb, D. T. and Kemphues, K. J. (1996). PAR-2 is asymmetrically distributed and promotes association of P granules and PAR-1 with the cortex in *C. elegans* embryos. *Development* **122**, 3075-3084.

Brenner, S. (1974). The Genetics of *Caenorhabditis elegans*. *Genetics* **77**, 71-94.

Brower, C. S., Sato, S., Tomomori-Sato, C., Kamura, T., Pause, A., Stearman, R., Klausner, R. D., Malik, S., Lane, W. S., Sorokina, I. et al. (2002). Mammalian mediator subunit mMED8 is an Elongin BC-interacting protein that can assemble with Cul2 and Rbx1 to reconstitute a ubiquitin ligase. *Proc. Natl. Acad. Sci. USA* **99**, 10353-10358.

Buonomo, S. B., Clyne, R. K., Fuchs, J., Loidl, J., Uhlmann, F. and Nasmyth, K. (2000). Disjunction of homologous chromosomes in meiosis I depends on proteolytic cleavage of the meiotic cohesin Rec8 by separin. *Cell* **103**, 387-398.

Chang, D. C., Xu, N. and Luo, K. Q. (2003). Degradation of cyclin B is required for the onset of anaphase in mammalian cells. *J. Biol. Chem.* **278**, 37865-37873.

Cooper, K. F., Mallory, M. J., Egeland, D. B., Jarnik, M. and Strich, R. (2000). Ama1p is a meiosis-specific regulator of the anaphase promoting complex/cyclosome in yeast. *Proc. Natl. Acad. Sci. USA* **97**, 14548-14553.

Cuenca, A. A., Schetter, A., Aceto, D., Kemphues, K. and Seydoux, G. (2003). Polarization of the *C. elegans* zygote proceeds via distinct establishment and maintenance phases. *Development* **130**, 1255-1265.

Davis, E. S., Wille, L., Chestnut, B. A., Sadler, P. L., Shakes, D. C. and Golden, A. (2002). Multiple subunits of the *Caenorhabditis elegans* anaphase-promoting complex are required for chromosome segregation during meiosis I. *Genetics* **160**, 805-813.

DeRenzo, C., Reese, K. J. and Seydoux, G. (2003). Exclusion of germ plasm proteins from somatic lineages by cullin-dependent degradation. *Nature* **424**, 685-689.

Epstein, A. C., Gleadle, J. M., McNeill, L. A., Hewitson, K. S., O'Rourke, J., Mole, D. R., Mukherji, M., Metzen, E., Wilson, M. I., Dhanda, A. et al. (2001). *C. elegans* EGL-9 and mammalian homologs define a family of dioxygenases that regulate HIF by prolyl hydroxylation. *Cell* **107**, 43-54.

Feng, H., Zhong, W., Punkosdy, G., Gu, S., Zhou, L., Seabolt, E. K. and Kipreos, E. T. (1999). CUL-2 is required for the G1-to-S phase transition and mitotic chromosome condensation in *Caenorhabditis elegans*. *Nat. Cell. Biol.* **1**, 486-492.

Fire, A., Xu, S., Montgomery, M. K., Kostas, S. A., Driver, S. E. and Mello, C. C. (1998). Potent and specific genetic interference by double-stranded RNA in *Caenorhabditis elegans*. *Nature* **391**, 806-811.

Furuta, T., Tuck, S., Kirchner, J., Koch, B., Auty, R., Kitagawa, R., Rose, A. M. and Greenstein, D. (2000). EMB-30: an APC4 homologue required for metaphase-to-anaphase transitions during meiosis and mitosis in *Caenorhabditis elegans*. *Mol. Biol. Cell* **11**, 1401-1419.

Goldstein, B. and Hird, S. N. (1996). Specification of the anteroposterior axis in *Caenorhabditis elegans*. *Development* **122**, 1467-1474.

Grill, S. W., Gonczy, P., Stelzer, E. H. and Hyman, A. A. (2001). Polarity controls forces governing asymmetric spindle positioning in the *Caenorhabditis elegans* embryo. *Nature* **409**, 630-633.

Hagting, A., den Elzen, N., Vodermaier, H. C., Waizenegger, I. C., Peters, J. M. and Pines, J. (2002). Human securin proteolysis is controlled by the spindle checkpoint and reveals when the APC/C switches from activation by Cdc20 to Cdh1. *J. Cell Biol.* **157**, 1125-1137.

Herbert, M., Levasseur, M., Homer, H., Yallop, K., Murdoch, A. and McDougall, A. (2003). Homologue disjunction in mouse oocytes requires proteolysis of securin and cyclin B1. *Nat. Cell. Biol.* **5**, 1023-1025.

Hung, T. J. and Kemphues, K. J. (1999). PAR-6 is a conserved PDZ domain-containing protein that colocalizes with PAR-3 in *Caenorhabditis elegans* embryos. *Development* **126**, 127-135.

Joberty, G., Petersen, C., Gao, L. and Macara, I. G. (2000). The cell-polarity protein Par6 links Par3 and atypical protein kinase C to Cdc42. *Nat. Cell. Biol.* **2**, 531-539.

Kamath, R. S., Fraser, A. G., Dong, Y., Poulin, G., Durbin, R., Gotta, M., Kanapin, A., Le Bot, N., Moreno, S., Sohrmann, M. et al. (2003). Systematic functional analysis of the *Caenorhabditis elegans* genome using RNAi. *Nature* **421**, 231-237.

Kamizono, S., Hanada, T., Yasukawa, H., Minoguchi, S., Kato, R., Minoguchi, M., Hattori, K., Hatakeyama, S., Yada, M., Morita, S. et al. (2001). The SOCS box of SOCS-1 accelerates ubiquitin-dependent proteolysis of TEL-JAK2. *J. Biol. Chem.* **276**, 12530-12538.

Kamura, T., Burian, D., Yan, Q., Schmidt, S. L., Lane, W. S., Querido, E., Branton, P. E., Shilatifard, A., Conaway, R. C. and Conaway, J. W. (2001). Muf1, a novel Elongin BC-interacting leucine-rich repeat protein that can assemble with Cul5 and Rbx1 to reconstitute a ubiquitin ligase. *J. Biol. Chem.* **276**, 29748-29753.

Kemphues, K. J., Wolf, N., Wood, W. B. and Hirsh, D. (1986). Two loci required for cytoplasmic organization in early embryos of *Caenorhabditis elegans*. *Dev. Biol.* **113**, 449-460.

Kim, W. and Kaelin, W. G., Jr (2003). The von Hippel-Lindau tumor

suppressor protein: new insights into oxygen sensing and cancer. *Curr. Opin. Genet. Dev.* **13**, 55-60.

Kitajima, T. S., Miyazaki, S., Yamamoto, A. and Watanabe, Y. (2003). Rec8 cleavage by separase is required for meiotic nuclear divisions in fission yeast. *EMBO J.* **22**, 5643-5653.

Nebreda, A. R. and Ferby, I. (2000). Regulation of the meiotic cell cycle in oocytes. *Curr. Opin. Cell Biol.* **12**, 666-675.

Nixon, V. L., Levasseur, M., McDougall, A. and Jones, K. T. (2002). Ca(2+) oscillations promote APC/C-dependent cyclin B1 degradation during metaphase arrest and completion of meiosis in fertilizing mouse eggs. *Curr. Biol.* **12**, 746-750.

O'Connell, K. F., Maxwell, K. N. and White, J. G. (2000). The *spd-2* gene is required for polarization of the anteroposterior axis and formation of the sperm asters in the *Caenorhabditis elegans* zygote. *Dev. Biol.* **222**, 55-70.

Ohta, T., Michel, J. J., Schottelius, A. J. and Xiong, Y. (1999). ROC1, a homolog of APC11, represents a family of cullin partners with an associated ubiquitin ligase activity. *Mol. Cell* **3**, 535-541.

Pasierbek, P., Jantsch, M., Melcher, M., Schleiffer, A., Schweizer, D. and Loidl, J. (2001). A *Caenorhabditis elegans* cohesion protein with functions in meiotic chromosome pairing and disjunction. *Genes Dev.* **15**, 1349-1360.

Pause, A., Peterson, B., Schaffar, G., Stearman, R. and Klausner, R. D. (1999). Studying interactions of four proteins in the yeast two-hybrid system: structural resemblance of the pVHL/elongin BC/hCUL-2 complex with the ubiquitin ligase complex SKP1/cullin/F-box protein. *Proc. Natl. Acad. Sci. USA* **96**, 9533-9538.

Pellettieri, J. and Seydoux, G. (2002). Anterior-posterior polarity in *C. elegans* and *Drosophila*-PARallels and differences. *Science* **298**, 1946-1950.

Peter, M., Castro, A., Lorca, T., Le Peuch, C., Magnaghi-Jaulin, L., Doree, M. and Labbe, J. C. (2001). The APC is dispensable for first meiotic anaphase in *Xenopus* oocytes. *Nat. Cell. Biol.* **3**, 83-87.

Peters, J. M. (2002). The anaphase-promoting complex: proteolysis in mitosis and beyond. *Mol. Cell* **9**, 931-943.

Petronczki, M., Siomos, M. F. and Nasmyth, K. (2003). Un Menage a Quatre. The Molecular Biology of Chromosome Segregation in Meiosis. *Cell* **112**, 423-440.

Pickart, C. M. (2001). Mechanisms underlying ubiquitination. *Annu. Rev. Biochem.* **70**, 503-533.

Pintard, L., Kurz, T., Glaser, S., Willis, J. H., Peter, M. and Bowerman, B. (2003a). Neddylation and deneddylation of CUL-3 is required to target MEI-1/Katanin for degradation at the meiosis-to-mitosis transition in *C. elegans*. *Curr. Biol.* **13**, 911-921.

Pintard, L., Willis, J. H., Willems, A., Johnson, J. L., Srayko, M., Kurz, T., Glaser, S., Mains, P. E., Tyers, M., Bowerman, B. et al. (2003b). The BTB protein MEL-26 is a substrate-specific adaptor of the CUL-3 ubiquitin-ligase. *Nature* **425**, 311-316.

Rogers, E., Bishop, J. D., Waddle, J. A., Schumacher, J. M. and Lin, R. (2002). The aurora kinase AIR-2 functions in the release of chromosome cohesion in *Caenorhabditis elegans* meiosis. *J. Cell Biol.* **157**, 219-229.

Sasagawa, Y., Urano, T., Kohara, Y., Takahashi, H. and Higashitani, A. (2003). *Caenorhabditis elegans* RBX1 is essential for meiosis, mitotic chromosomal condensation and segregation, and cytokinesis. *Genes Cells* **8**, 857-872.

Schneider, S. Q. and Bowerman, B. (2003). Cell polarity and the cytoskeleton in the *Caenorhabditis elegans* zygote. *Annu. Rev. Genet.* **37**, 221-249.

Shelton, C. A. and Bowerman, B. (1996). Time-dependent responses to *glp-1*-mediated inductions in early *C. elegans* embryos. *Development* **122**, 2043-2050.

Siomos, M. F., Badrinath, A., Pasierbek, P., Livingstone, D., White, J., Glotzer, M. and Nasmyth, K. (2001). Separase is required for chromosome segregation during meiosis I in *Caenorhabditis elegans*. *Curr. Biol.* **11**, 1825-1835.

Stemmann, O., Zou, H., Gerber, S. A., Gygi, S. P. and Kirschner, M. W. (2001). Dual inhibition of sister chromatid separation at metaphase. *Cell* **107**, 715-726.

Strome, S. and Wood, W. B. (1982). Immunofluorescence visualization of germ-line-specific cytoplasmic granules in embryos, larvae, and adults of *Caenorhabditis elegans*. *Proc. Natl. Acad. Sci. USA* **79**, 1558-1562.

Strome, S. and Wood, W. B. (1983). Generation of asymmetry and segregation of germ-line granules in early *C. elegans* embryos. *Cell* **35**, 15-25.

Tabuse, Y., Izumi, Y., Piano, F., Kemphues, K. J., Miwa, J. and Ohno, S. (1998). Atypical protein kinase C cooperates with PAR-3 to establish embryonic polarity in *Caenorhabditis elegans*. *Development* **125**, 3607-3614.

Timmons, L., Court, D. L. and Fire, A. (2001). Ingestion of bacterially expressed dsRNAs can produce specific and potent genetic interference in *Caenorhabditis elegans*. *Gene* **263**, 103-112.

Tyers, M. and Jorgensen, P. (2000). Proteolysis and the cell cycle: with this RING I do thee destroy. *Curr. Opin. Genet. Dev.* **10**, 54-64.

Uhlmann, F., Wernic, D., Poupart, M. A., Koonin, E. V. and Nasmyth, K. (2000). Cleavage of cohesin by the CD clan protease separin triggers anaphase in yeast. *Cell* **103**, 375-386.

Wallenfang, M. R. and Seydoux, G. (2000). Polarization of the anterior-posterior axis of *C. elegans* is a microtubule-directed process. *Nature* **408**, 89-92.

Watts, J. L., Etemad-Moghadam, B., Guo, S., Boyd, L., Draper, B. W., Mello, C. C., Priess, J. R. and Kemphues, K. J. (1996). *par-6*, a gene involved in the establishment of asymmetry in early *C. elegans* embryos, mediates the asymmetric localization of PAR-3. *Development* **122**, 3133-3140.

Wittmann, T., Hyman, A. and Desai, A. (2001). The spindle: a dynamic assembly of microtubules and motors. *Nat. Cell. Biol.* **3**, E28-E34.